

## Tapping into our blood: Age-gender associated protein in human blood plasma and its potential relevance in skin aging

**Florence<sup>1\*</sup>, Masatoshi Haga<sup>1</sup>, Yasunari Sato<sup>1</sup>**

<sup>1</sup>Basic Research Development Division, ROHTO Pharmaceutical Co., Ltd., Kunimidai, Kizugawa, Kyoto, Japan

\*Florence

ROHTO PHARMACEUTICAL CO., LTD.

6-5-4, Kunimidai, Kizugawa, Kyoto 619-0216, Japan

E-mail: florence@rohto.co.jp

Tel: +81-774-71-8772 Fax: +81-774-71-8781

### Abstract

This study describes, for the first time, the potential biological effect of the female-age-associated plasma protein osteomodulin (OMD) on the skin. Despite extensive skin microcirculation, how changes in circulating plasma proteins influence the skin is still not well studied. Using 3K SOMAscan proteomics measurements from 3,301 human plasma samples from the INTERVAL cohort (Cambridge, UK), we found a cluster of eight plasma proteins whose detection across age increased differently in females than in males. Among these proteins, OMD was selected for further evaluation because of its previous report on interaction with type I collagen. The result of type I collagen immunostaining showed disruption of collagen fibrils in cultured human dermal fibroblasts upon addition of OMD. Furthermore, 0.1 µM and 1 µM OMD potentially inhibited the association of collagen fiber formation, resulting in a shift of the collagen fibril diameter distribution to thinner fibrils. OMD reduced the expression of *OCLN* and *KRT1* genes in cultured human keratinocytes, suggesting that OMD might play a role in the induction of epidermal and barrier function disruption. Lastly, an increase in transepidermal water loss after 5 days of OMD treatment in the human skin equivalent (HSE) model was observed, which caused an aberrant distribution of *KRT1* concentrated at the top of the suprabasal epidermis. Taken together, our findings indicate that OMD has the potential to affect the epidermis and dermis of the skin. Using OMD as a target, we can potentially improve both dermal and epidermal concerns during aging.

**Keywords:** plasma protein; intrinsic aging; osteomodulin; extracellular matrix; epidermal differentiation; epidermal barrier function

### Abbreviations

OMD	Osteomodulin
TEWL	Transepidermal water loss
Ctrl	Control group (untreated with OMD)
COL1A1	Type 1 collagen alpha chain 1
CLDN1	Claudin 1
OCLN	Occludin
KRT1	Keratin 1

KRT14	Keratin 14
FLG	Filaggrin
LOR	Loricrin
IVL	Involucrin
HSE	Human Skin Equivalent

## Introduction

Previous research on parabiosis between young and old mice, such that they share a circulatory system, reported that factors present in young serum has regenerative effects on tissues and organs of old mice, while degenerative effects were seen in the organs of young mice due to factors from old serum [1]. This leads to the interesting hypothesis that age-related molecular changes in blood could contribute to organismal aging [2].

Skin aging is a multifaceted process that is influenced by various intrinsic factors (e.g., cellular senescence) and extrinsic factors (e.g., UV rays, irritants) [3]. Despite extensive skin microcirculation, how changes in circulating plasma proteins influence the skin is still not well studied. The upper skin microcirculation is located in the papillary dermis with capillary loops that extend perpendicular to the skin surface, in proximity to the epidermal basal layer [4]. The regulation of blood vessel permeability is essential for the homeostasis of peripheral tissues. Cutaneous blood vessels act as a barrier of approximately 70 kDa, presumably allowing the passive diffusion of small molecules, including ions, glucose, urea, amino acids, insulin, cytokines, small proteins, amyloids, and some hormones, but does not allow the diffusion of albumin (66 kDa), transferrin (80 kDa), and immunoglobulins (> 100 kDa) [5].

Blood proteins below 66 kDa, such as HBG1 (Hemoglobin Subunit Gamma 1, 14–16 kDa), as well as some bone-specific proteoglycans that are not highly expressed in the skin, such as osteomodulin (OMD, 49 kDa) and osteoglycin (OGN, 34 kDa), can be found in the skin tissue, supporting the above study [6]. We hypothesized that aging-related blood plasma proteins smaller than 66 kDa may interact with neighboring skin cells and contribute to the skin aging process, which may shed new light on intrinsic skin aging factors.

In the present study, we aimed to identify candidate blood proteins that change according to both age and sex as potential intrinsic factors in skin aging and to evaluate their biological effects on the skin. We focused on age-related molecular changes in the blood that might contribute specifically to female or male skin aging.

## Results

### ***Increase of OMD and several other blood proteins in females aged 45-50 years, but not in males.***

We clustered 3,283 plasma proteins from 3,301 healthy individuals (1,616 females and 1,685 males) aged 18–76 years from the INTERVAL cohort [7][8] (Fig. 1A) and visualized them as z-scored changes across the lifespan. We observed that most blood proteins did not show any dramatic changes across 18–76 years of age (Fig. 1B). Interestingly, our heatmap visualization indicated a unique group of proteins within a cluster whose dynamics differed between females

and males, in which there was a clear change from negative z-score to positive z-score with increasing age in females (Fig. 1B). This cluster consisted of 8 proteins (Fig. 1C, Tab. 1): OMD, chondroadherin (CHAD), collagen type XI alpha 2 chain (COL11A2), leucine-rich repeat-containing protein 15 (LRRC15), glycoprotein hormones alpha chain/ choriogonadotropin subunit beta 3/ choriogonadotropin subunit beta 7 (CGA.CGB3.CGB7), lutropin subunit beta (LHB), CGA.LHB, glycoprotein hormones alpha chain/ follitropin subunit beta (CGA.FSHB). In females, this group of proteins showed a decreasing tendency at approximately 20–40 years of age, followed by a sudden increase at approximately 45–55 years. However, this unique dynamic was not observed in males, as these proteins either show an increase in abundance around age of 65 years or a gradual decrease across age (Fig. 1D).

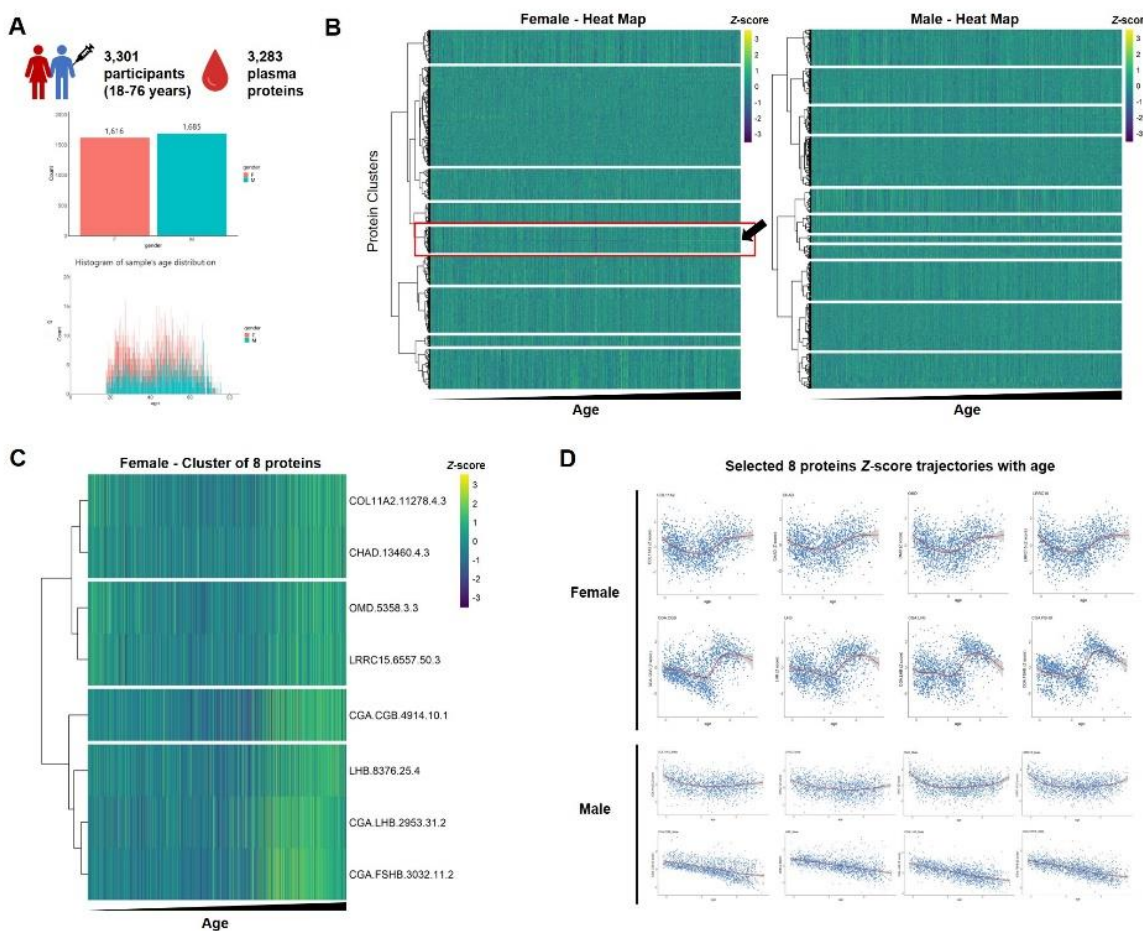


**Figure 1.** Clustered heatmap visualization of INTERVAL cohort plasma proteins. (A) Data demographics of 3,301 participants in the INTERVAL cohort. (B) Unsupervised hierarchical clustering and clustered heatmap were used to group plasma proteins with similar trajectories across all ages in females and males. The red rectangle pointed to the unique group of proteins within a cluster, which showed a change from negative z-score to positive z-score with increasing age in females. (C) Group of proteins represented by the red rectangle consist of eight plasma proteins. (D) Eight plasma proteins z-score trajectories across ages in females and males. Trajectories were estimated by LOESS.

Protein Name	Gene (Entrez Gene ID)	UniProt ID	Size (kDa)	GO Biological Processes	GO Molecular Function	GO Cellular Component
Collagen type XI alpha 2 chain	COL11A2	P13942	172	Cartilage development, collagen fibril organization	Extracellular matrix structural constituent, extracellular matrix structural constituent conferring tensile strength, metal ion binding, protein-macromolecule adaptor activity	Collagen trimer, collagen type XI trimer2, collagen-containing, endoplasmic reticulum lumen, extracellular matrix, extracellular region, extracellular space
Chondroadherin	CHAD	O15335	40	Bone development, negative regulation of bone trabecula formation	-	Extracellular matrix, extracellular space
Osteomodulin	OMD	Q99983	49	Regulation of bone mineralization, cell adhesion	-	Collagen-containing extracellular matrix, extracellular region, extracellular space, Golgi lumen, lysosomal lumen, extracellular exosome
Leucine-rich repeat-containing protein 15	LRRC15	Q8TF66	64	Negative regulation of protein localization to plasma membrane, positive regulation of cell migration, receptor-mediated virion attachment to host cell	Collagen binding, fibronectin binding, laminin binding	Extracellular exosome, extracellular matrix, extracellular space, integral component of membrane
Glycoprotein hormones alpha chain/choriogonadotropin subunit beta 3/choriogonadotropin subunit beta 7	CGA.CGB3.CGB7	P01215 (CGA) P0DN87 (CGB7)	~27	Developmental growth, follicle-stimulating hormone secretion, follicle-stimulating hormone signaling pathway, G protein-coupled receptor signaling pathway, hormone-mediated signaling pathway, luteinizing hormone secretion, negative regulation of organ growth, positive regulation of cell migration, positive regulation of cell population proliferation, positive regulation of steroid biosynthetic process, positive regulation of transcription by RNA polymerase II, regulation of signaling receptor activity, thyroid gland development, thyroid hormone generation	Follicle-stimulating hormone activity, hormone activity	Extracellular region, extracellular space, follicle-stimulating hormone complex, Golgi lumen, pituitary gonadotropin
Lutropin subunit beta	LHB	Q8WXL0	14	-	Hormone activity	Extracellular region
Glycoprotein hormones alpha chain/lutropin subunit beta	CGA.LHB	Q8WXL0 (LHB)	~27	Similar with CGA.CGB and LHB	Similar with CGA and LHB	Similar with CGA.CGB and LHB
Glycoprotein hormones alpha chain/ follitropin subunit beta	CGA.FSHB	P01225 (FSHB)	~27	female gamete generation, female pregnancy, follicle-stimulating hormone signaling pathway, G protein-coupled receptor signaling pathway, positive regulation of bone resorption, positive regulation of cell migration, positive regulation of cell population proliferation, positive regulation of gene expression, positive regulation of steroid biosynthetic process, positive regulation of transcription by RNA polymerase II, progesterone biosynthetic process, regulation of osteoclast differentiation, regulation of signaling receptor activity, Sertoli cell proliferation, spermatogenesis, transforming growth factor beta receptor signaling pathway	-	Cytoplasm, extracellular region, extracellular space, follicle-stimulating hormone complex, follicle-stimulating hormone activity

Gene IDs are obtained from the Entrez Gene resource of the NCBI. The biological process, molecular functions, and cellular component information is obtained from the Gene Ontology (GO) database.

**Table 1.** Gene ontology of eight proteins with unique dynamics across all ages in females.

Furthermore, we investigated the possible influence of these proteins on skin. We filtered through their molecular weight, as only proteins with sizes below 66 kDa can pass through skin blood vessels to skin tissue [5]. We also collected data on the previously reported functions of these proteins in cells and tissues. We found that OMD (Fig. 2), with a size of 49 kDa, was previously reported to interact with collagen type I and influence its fibrillogenesis [9]. OMD belongs to the family of small leucine-rich proteins (SLRPs), which are known to influence TGF- $\beta$  signaling and the skin matrisome. Thus, OMD was selected for further investigation.

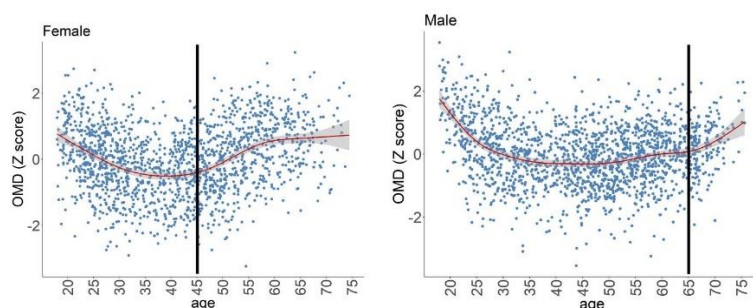


**Figure 2.** Osteomodulin (OMD). OMD trajectories across all ages in INTERVAL cohort. Black bar indicated time point of increasing trajectory.

**OMD disrupted type I collagen production and potentially exerted its regulatory effect on collagen fibrils association resulting in aberrant collagen fibrils in cultured human dermal fibroblast.**

OMD was previously reported to inhibit collagen gel fibrillogenesis [9]; however, whether it affects collagen fibrils *in-vitro* has not yet been established. To investigate this, we performed immunostaining for type I collagen and enzyme-linked immunosorbent assay (ELISA) for pro-collagen I alpha 1 in OMD-treated cultured normal human fibroblasts (NHDF). Type I collagen was stained in the extracellular compartment, and the staining intensities were lower in fibroblasts treated with 1 and 5  $\mu$ M OMD (Fig. 3A). Moreover, ELISA results showed a decrease in pro-collagen I production at 1  $\mu$ M OMD and abrupt production at 5 $\mu$ M OMD (Fig. 3B). Tashima *et al.* also observed a regulatory effect of OMD on collagen fibril diameter [9]. We investigated this regulatory effect using scanning electron microscopy (SEM), and the results showed that 0.1  $\mu$ M and 1  $\mu$ M OMD potentially inhibited the association of collagen, resulting in a shift of the collagen fibril diameter distribution to thinner fibrils (Fig. 3C, D).

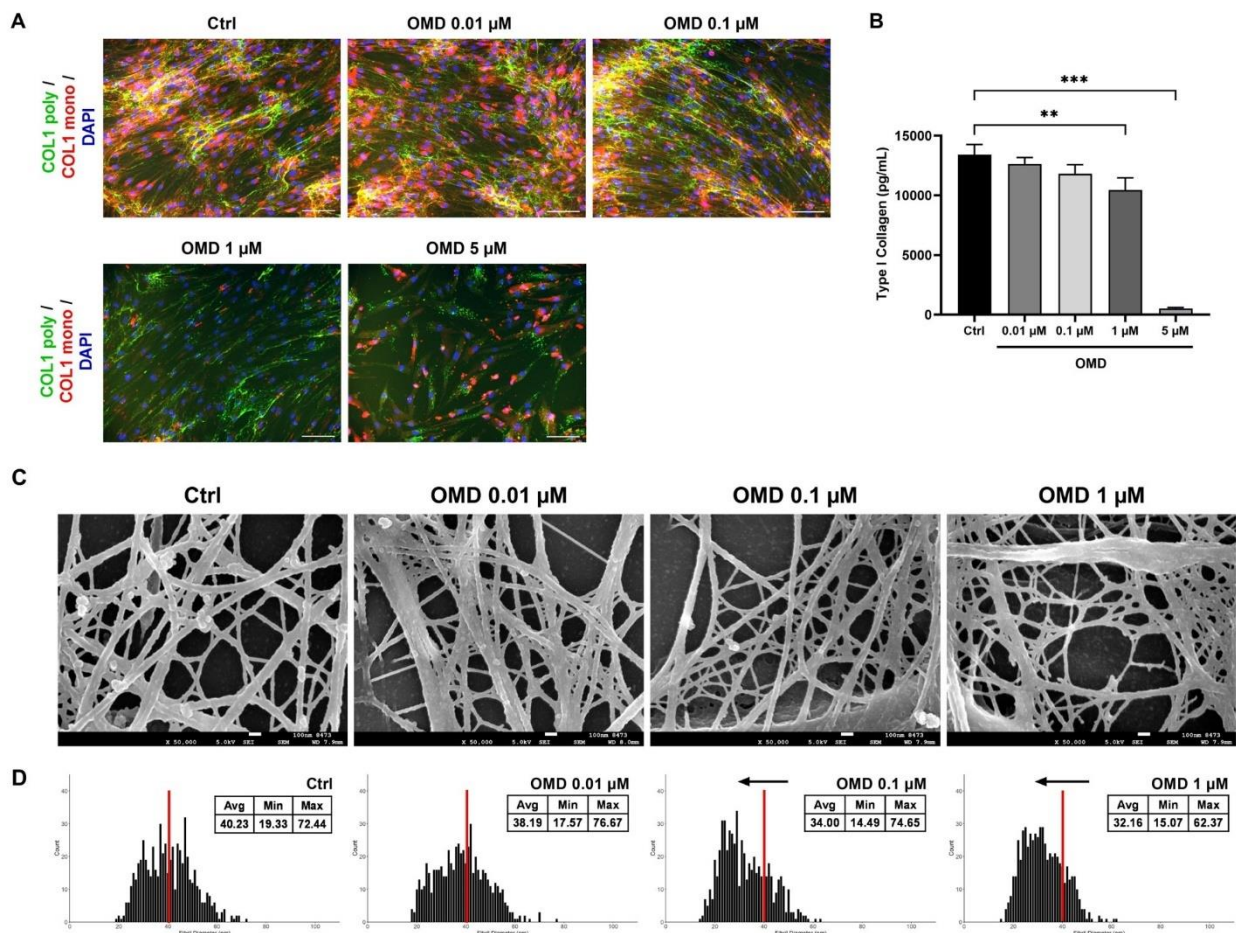


**Figure 3.** OMD disrupted type I collagen formation in cultured normal human dermal fibroblast (NHDF). (A) Representative immunofluorescence images of type 1 collagen fibrils of NHDF cells after 6 days in culture with 1mg/ml L-ascorbic acid and OMD. Control (Ctrl) group is not treated with OMD. (B) The amount of collagen type I was measured with ELISA kit. Collagen amount were normalized with number of viable cells. Values are presented as the mean  $\pm$  SD (n=3), vs control \*\* $p$  < 0.01, \*\*\* $p$  < 0.001 (Dunnett's Test). (C) Scanning electron microscopy images of NHDF extracellular matrix after treatment with OMD. (D) Quantification and distribution of collagen fibril diameters from control and OMD treated NHDF. The frequency of collagen fibrils with a given diameter is shown in the histogram. At least 600

fibrils from each treatment group images were used for the analysis. Collagen fibrils smaller than 40 nm in diameter (the left side of red line) had a higher frequency in OMD-treated NHDF. Scale bars: 100  $\mu$ m for A, 100 nm for C.

### **Reduced expression level of Keratin 1 and Occludin in OMD-treated cultured human keratinocytes.**

OMD was reported to alter the expression levels of tight junction genes in bladder cancer cell lines by inhibiting epidermal growth factor receptor (EGFR) signaling [10]. Thus, we investigated the influence of OMD on cultured human keratinocytes, focusing on epidermal differentiation and tight junction genes, which are strongly influenced by EGFR signaling. The expression of *OCLN* genes was lower in 0.1  $\mu$ M and 1  $\mu$ M OMD-treated keratinocytes than that in the control group (Fig. 4A), while decreasing tendency was observed for *CLDN1* and *LOR* (Fig. 4B, D). No significant difference was observed for *FLG* (Fig. 4C). Epidermal differentiation marker *KRT1* gene expression was significantly reduced upon treatment with 1  $\mu$ M OMD (Fig. 4E). This suggests that OMD may play a role in the induction of epidermal and barrier function disruption. We also conducted a lactate dehydrogenase (LDH) release assay to assess the possibility of cytotoxicity upon the addition of OMD to cultured human dermal fibroblasts and keratinocytes. The results showed no significant LDH release compared with that in the control group (Supplementary Fig. 1).

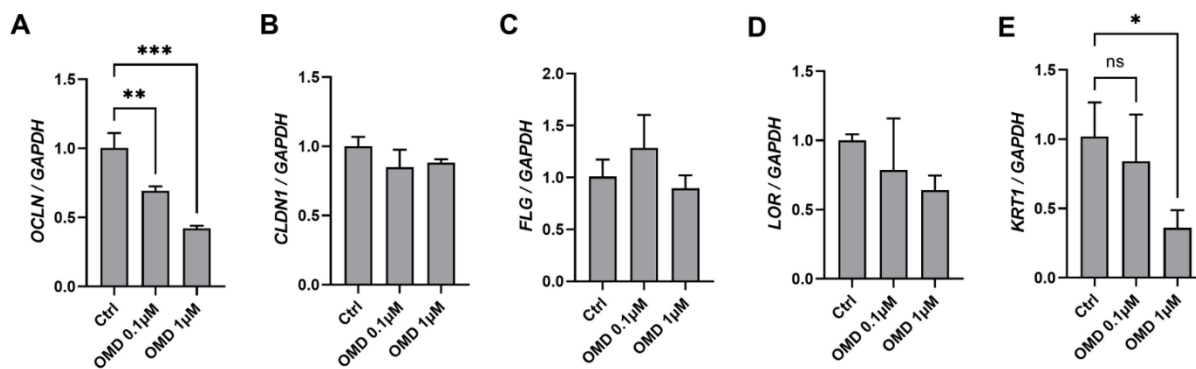
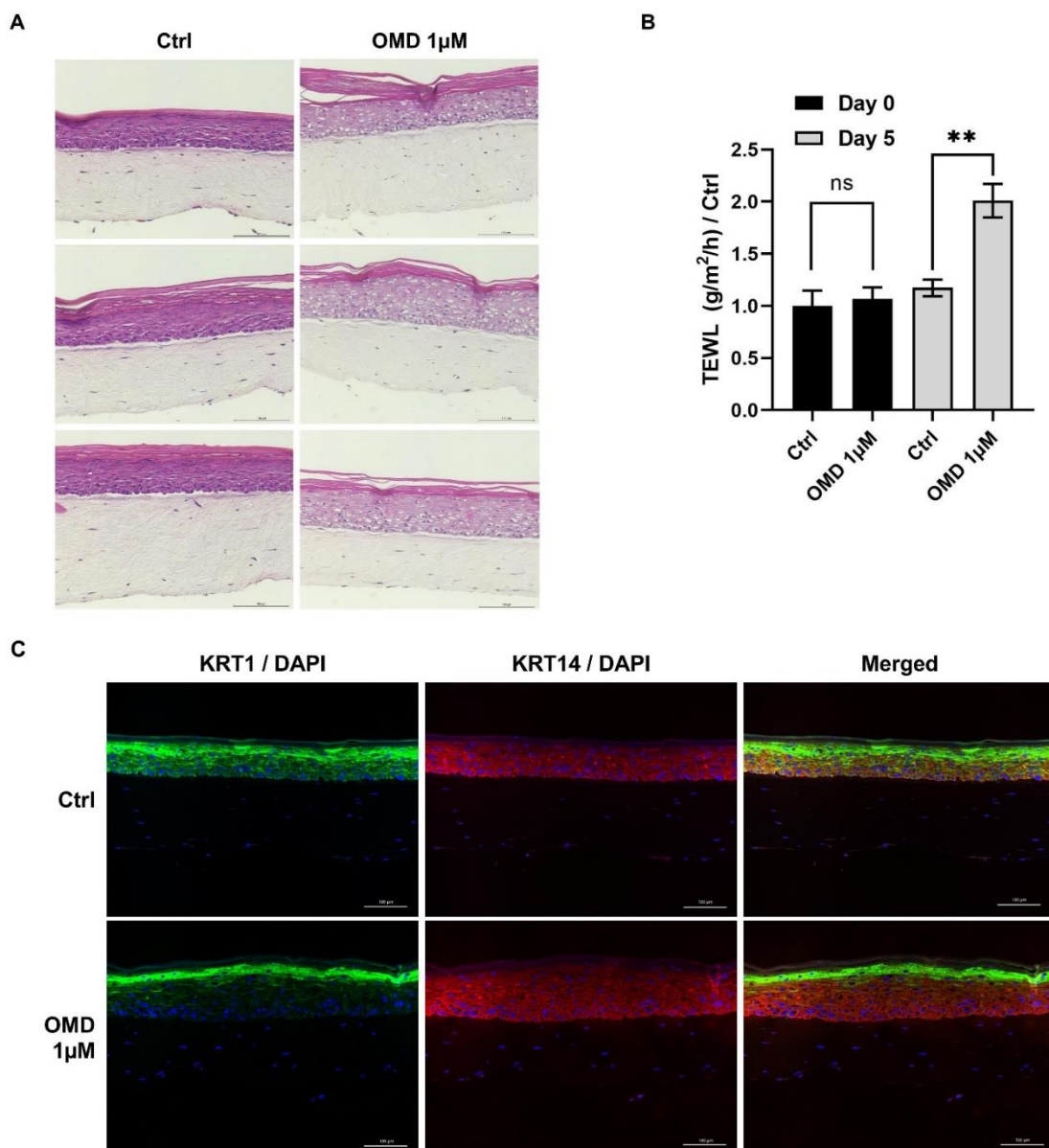


**Figure 4.** OMD-treated cultured normal human keratinocytes (NHEK). Gene expression of tight junction genes *OCLN*, *CLDN1* (A, B), terminal differentiation marker *FLG*, *LOR* (C, D), epidermal differentiation marker *KRT1* (E). *GAPDH* was used as a reference gene. Values are presented as the mean  $\pm$  SD (n=3). Dunnett's test, \*p < 0.05, \*\*p < 0.01, \*\*\*p < 0.001.

### **Disruption in epidermal differentiation is shown by aberrant distribution of *KRT1* and *FLG*, as well as high transepidermal water loss (TEWL) following treatment of OMD in skin equivalent model.**

To further investigate the effects of OMD on skin, we cultured a human skin equivalent (HSE) model with 1  $\mu$ M OMD containing medium for 5 days, and performed hematoxylin and eosin (H&E) staining, followed by TEWL measurements. Epidermal thickening was observed in OMD-treated HSE, with an increased number of perinuclear vacuole-like structures observed around the cell nucleus (Fig. 5A). An increase in TEWL was observed after 5 days of treatment with OMD (Fig. 5B), indicating disrupted epidermal barrier function. We performed immunostaining to further investigate the possible mechanisms of OMD disruption to barrier function. Treatment with OMD caused an aberrant distribution of *KRT1*, concentrated at the top of the suprabasal epidermis,

with a gradient distribution in the control group (Fig. 5C). Differences in protein distribution were also observed with FLG/CLDN1 immunostaining, with OMD-treated HSE showing an overlapping stained area on the stratum granulosum, while the control group showed clearer separation in the stained area between FLG and CLDN1 (Fig. 5D). In addition, a reduction of Ki67 positive cells in OMD-treated HSE was also observed, indicating that the proliferation of cells in the basal layer was reduced (Fig. 5E). Furthermore, the expression level of *KRT1* was significantly reduced in OMD-treated HSE, whereas the terminal differentiation genes *FLG*, *LOR*, and tight junction genes *OCLN* only showed a decreasing tendency (Fig. 5F). Taken together, these results indicate that exposure of the skin to OMD could possibly lead to disruption of skin barrier function. Additionally, we investigated expression level of *COL1A1* from HSE dermis, and found a significant reduction in OMD-treated HSE (Fig. 5G).



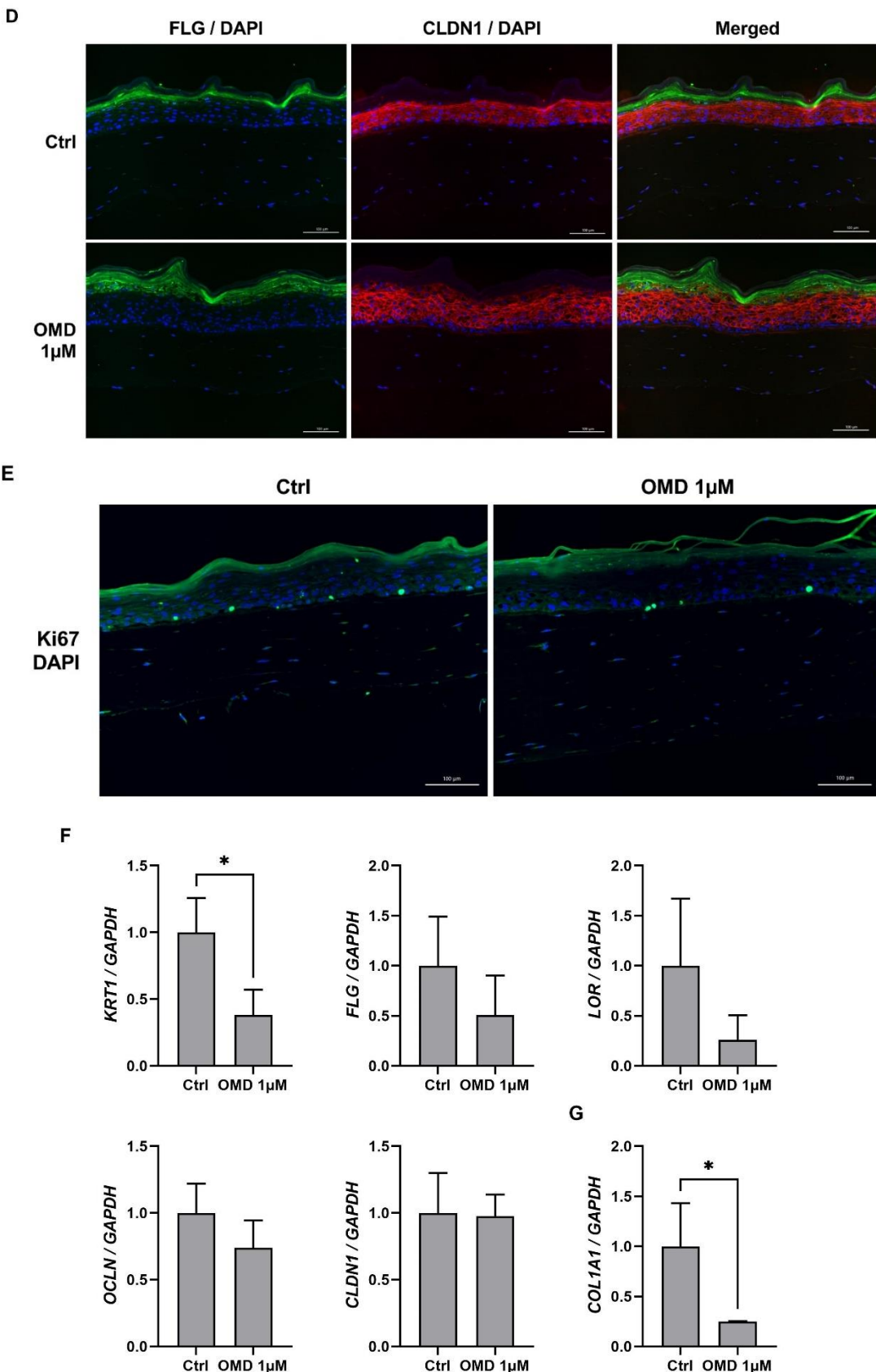


**Figure 5.** Histological analysis of OMD-treated human skin equivalent (HSE). (A) H&E staining of HSE after 5 days of culture with 1  $\mu$ M OMD. Scale bars, 100  $\mu$ m. Difference in epidermis structure could be observed. (B) Transepidermal water loss (TEWL) was measured before and after 5 days of treatment with OMD. Triplicate measurement for each HSE was taken and averaged. Immunostaining of KRT1/KRT14 (C), FLG/CLDN1 (D), and Ki67 (E) of HSE after 5 days of treatment with 1  $\mu$ M OMD compared with that of the control. (F) Gene expression of *KRT1*, *FLG*, *LOR*, *OCLN*, and *CLDN1* in epidermis of HSE. (G) Gene expression of *COL1A1* in dermis of HSE. GAPDH was used as a reference gene. All values are presented as the mean  $\pm$  SD (n=3). Student's t-test, \* $p$  < 0.05, \*\* $p$  < 0.01. Scale bars: 100  $\mu$ m for A, C, D and E.

## Discussion

This study describes, for the first time, the potential biological effect of the female-age-associated plasma protein OMD on the skin. Cellular senescence and hormonal changes are common causes of intrinsic aging of the skin, which are usually investigated in the search for solutions. Here, we describe additional factors in the blood plasma that potentially contribute to the skin aging process.

By separately analyzing the plasma proteome data of males and females from the INTERVAL cohort, we were able to identify eight proteins that have different dynamics between genders. Among these, OMD was selected based on a previous report[9] on its interaction with type I collagen. In Fig. 2, we can see how OMD abundance in the blood starts to increase in females aged 45–55 years. This increase was seen at a later age in males, approximately 75 years of age.

OMD is highly expressed in mineralized tissues such as bones and teeth, and has been reported to positively regulate osteogenesis [11][12]. Previous reports stated that during perimenopausal (approximately 40–45 years) and menopausal (approximately 50 years) stage, lower estrogen levels results in increased bone loss and risk of osteoporosis [13]. Increasing osteoclastic activity of our bone with the decrease of systemic estrogen level during menopause [14], might contribute to elevated abundance of bone proteins released to the circulatory system. Additionally, *OMD* gene expression in the mammary glands of mice was suppressed in the presence of estrogen [15]. Therefore, we suspect a correlation between estrogen-influenced changes in the female body and an increase in OMD levels in blood plasma. Moreover, female skin condition changes dramatically during perimenopausal period from reduced matrisome production to skin dryness [16][17]. Our results showed that OMD reduced the epidermis barrier function (Fig. 5B) and disrupted collagen production and collagen fibrils (Fig. 3A, B, D). The correlation between OMD detection level, estrogen level, and menopausal skin changes should be explored in future studies with larger data points in menopausal women.

As reported in a previous study, OMD binds to type I collagen and may slow the collagen fibril association [9]. Our present findings showed that this phenomenon was also observed in cultured human fibroblasts, with reduced collagen production in 1  $\mu$ M OMD-treated group. In addition, treatment with 1  $\mu$ M and 5  $\mu$ M OMD altered the shape of dermal fibroblasts to an elongated shape. However, the expression level of senescence marker p21 did not increase with OMD treatment. We speculate that the change in fibroblast shape is either due to the loss of extracellular collagen or irregular cell cytoskeleton signaling. Interestingly, OMD also influenced collagen fibril assembly and thus collagen fibril diameter, which may contribute to the reduction of type 1 collagen quality. In SPARC-null mice, whose dermis displays abnormalities with decreased collagen fibril diameter,

skin laxity, and sensitivity to tearing were observed [18], which suggests a possible phenotype of skin with decreased collagen fibril diameter. A significantly higher value of skin extensibility or high skin laxity has also been observed in menopausal skin compared with that of nonmenopausal skin [19]. OMD could potentially be involved in this process by affecting collagen diameter. Although extrinsic aging (sun exposure) is the main driving force of the decrease in collagen quantity during aging skin; Interestingly, intrinsic aging plays a more central role in changes in collagen quality, such as orientation [20] and fiber width [21][22]. Taken together, our results showed that the plasma protein OMD is potentially able to drive changes in collagen quality and quantity in the skin. However, reduction of type 1 collagen staining intensity in the OMD-treated HSE model was not observed (data not shown), possibly due to the low production level of type 1 collagen in non-stimulated HSE fibroblasts. The addition of ascorbic acid to HSE could help us better evaluate the difference in collagen production levels.

One of the major interests of our study was how OMD affects epidermal barrier function in HSE, as well as epidermal differentiation and tight junction gene expression in cultured keratinocytes. It is intriguing to observe how OMD in HSE culture medium, which does not have direct contact with the epidermis, exerts its influence on epidermal physiology and barrier function. H&E staining revealed perinuclear vacuole-like structures around the nucleus of keratinocytes (Fig. 5A), as well as thickening of the epidermal layer. This perinuclear vacuole-like structure also appears when cells are exposed to toxicant [23] and UV-rays. However, the LDH assay analysis showed that OMD 1  $\mu$ M was not toxic to cultured fibroblasts, keratinocytes, and HSE models (Supplementary Fig.1). Whether this perinuclear vacuole-like structure plays an important role in the mechanism of action of OMD requires further investigation. In addition, a reduction of Ki67 positive cells in OMD-treated HSE was also observed, indicating a reduction of proliferating cells in the basal layer, which is one of the signs of intrinsic aging (Fig. 5E). Furthermore, the aberrant distribution of KRT1 (Fig. 5C) suggested the involvement of reduced KRT1 production levels in the observed H&E staining phenotype. KRT1 is an integral protein that maintains skin epidermal integrity and participates in inflammatory cytokine networks [24]. KRT1 downregulation has been correlated with an increase in the inflammatory cytokine IL-18 in the murine epidermis [24]. Despite the high TEWL of the OMD-treated HSE model, significant reductions in FLG gene expression levels and staining intensities were not observed (Fig. 5D, F), despite FLG being an integral protein in maintaining the skin barrier function. Although we were not able to explain the biological consequences of the difference in the distribution of FLG and CLDN1 immunostaining between the control and OMD-treated groups (Fig. 5D), this difference is a possible indication of the OMD mechanism of action towards the epidermis.

Loss of the skin's most abundant matrisome, type 1 collagen quantity, and quality, affect the appearance of the skin, resulting in fine wrinkles and sagging. Skin dryness is also a major concern in aging skin, especially menopausal skin, causing discomfort and fragile barrier function. The above findings indicate that OMD has the potential to influence both the epidermis and dermis of the skin (Fig. 3-5). OMD has been reported to bind to receptors and block common ligands in fibroblasts and keratinocytes, such as EGFR, epidermal growth factor (EGF), and transforming growth factor beta (TGF- $\beta$ ). Further investigations are necessary to elucidate the exact mechanism of action of OMD.

## Conclusion

Using OMD as a target, we are potentially able to tackle both dermal and epidermal concerns of aging by locally transmitting OMD inhibiting ingredients on the skin. Lastly, in this study, we only investigated the biological effects of OMD on the skin and intrinsic skin aging. As blood circulates through the whole body and different parts of peripheral organs, further studies on how OMD affects other peripheral organs, such as the eyes and muscles, are necessary.

## Materials and Methods

### INTERVAL cohort

3K SOMAscan proteomics z-scored measurements of 3,283 plasma proteins from 3,301 human plasma samples (1,685 males and 1,616 females) from the INTERVAL cohort (Cambridge, UK) were used for this study, with ages ranging from 18-76 years and a median age of 45 years. The INTERVAL data are available from the European Genome-Phenome Archive under the accession number EGAS00001002555.

### INTERVAL cohort data analysis

Proteins with similar dynamics across human lifespan were clustered and visualized as z-scored changes using the R pheatmap package (version 1.0.12). Male and female data were analyzed separately, and the protein cluster that showed an increase in detection level with increasing age in females, but not in males, was isolated. Proteins were selected based on their potential association with skin in previous studies.

### Cell cultures and materials

For cultured human dermal fibroblasts, neonatal normal human dermal fibroblasts (NHDFs (NB)), lot no. 05882 (Kurabo, Osaka, Japan) were used and cultured in Dulbecco's modified Eagle's medium (DMEM; Gibco, USA) supplemented with 10% fetal bovine serum and 1% antibiotic-antimycotic. For cultured human keratinocytes, neonatal normal human epidermal keratinocytes (NHEK (NB)), lot no. 7609 (Kurabo, Osaka, Japan), were used and cultured in Humedia-KG2 medium (Kurabo, Japan). All the cells were incubated in a 5% CO<sub>2</sub> incubator at 37 °C. Recombinant human OMD (ab27632) was obtained from Abcam (Cambridge, UK). The pro-collagen 1 ELISA kit (Human Pro-Collagen I alpha 1 DuoSet ELISA, DY6220-05) was purchased from R&D Systems (Minneapolis, MN, USA). Viable cells were stained with Hoechst 33342 (Dojindo, Kumamoto, Japan), and counted with ImageXpress® (Molecular Devices, California, USA). All additional supplies and reagents were routinely available.

### Human skin equivalent (HSE) model

HSE model (T-skinTM) and medium were purchased from EPISKIN SA (Lyon, France). The HSE model was cultured in the presence or absence of 1 µM OMD for five days. After 5 days, the samples were fixed in 4% paraformaldehyde phosphate buffer solution (Fujifilm Wako Pure Chemical Corporation, Osaka, Japan) and embedded in paraffin for H&E staining and immunostaining. For quantitative real-time polymerase chain reaction (RT-PCR), the epidermis and dermis of HSE were separated with clean forceps. Prior to RNA extraction, the tissues were

mashed with BiomasherII (Nippi, Tokyo, Japan) and centrifuged for 10 min at 10,000 × g. The supernatant was used for extraction with an RNeasy Mini Kit (Qiagen, Hilden, Germany).

### **Immunohistochemistry**

NHDF were plated at a density of 38,000 cells per well in 24-well plates and cultured overnight in DMEM supplemented with 10% fetal bovine serum and 1% antibiotic-antimycotic. The following day, the medium was replaced with DMEM (without fetal bovine serum) supplemented with 1% antibiotic-antimycotic and 1 mg/ml L-ascorbic acid (013-12061, Fujifilm Wako Pure Chemical Corporation, Osaka, Japan). Recombinant OMD (0.01 µM, 0.1 µM, 1, or 5 µM) was added to the treatment group. After treatment for 6 days, the cells were washed with PBS and incubated with primary antibodies targeting type I collagen (C2456, monoclonal, Sigma-Aldrich, Missouri, USA and NB600-408, polyclonal, Novus Biologicals, Colorado, USA) overnight at 4 °C. Primary antibodies were detected using Alexa488- or Alexa546-conjugated secondary antibodies and incubated for 1 h 37 °C incubation.

HSE tissue sections were incubated for 2 h at 37 °C with primary antibodies targeting Ki67 (ab16667, Abcam, Cambridge, UK), KRT1 (ab185628, Abcam), KRT14 (ab7800, Abcam), FLG (ab17808, Abcam), and CLDN1 (ab211737, Abcam). Primary antibodies were detected using Alexa488- or Alexa594-conjugated secondary antibodies and incubated for 1 h at 37 °C (Thermo Fisher Scientific, Waltham, MA, US). Samples were examined, and images were captured using an all-in-one fluorescence microscope BZ-X800 (Keyence, Osaka, Japan).

### **Scanned electron microscope (SEM)**

NHDFs were plated using a protocol similar to that sample. Recombinant OMD (0.01 µM, 0.1 µM, or 1 µM) was added to the treatment group. After treatment for 6 days, NHDF were fixed with fixation solution, and samples were submitted for SEM observation.

### **Quantitative real-time RT-PCR**

RNAs was extracted from cultured cells using an RNeasy mini kit (Qiagen, Hilden, Germany), and RNA concentration was determined using a NanoDrop UV-Vis spectrophotometer (Thermo Fisher Scientific, Massachusetts, US). For qPCR, RNAs were reverse-transcribed into first-strand cDNA using ReverTraAce qPCR RT Master Mix (Toyobo, Osaka, Japan). The cDNA was mixed with SYBR™ Green PCR Master Mix and primers for KRT1, KRT10, OCLN, CLDN1, FLG, LOR, IVL, KRT1, KRT10, COL1A1, p21, and OMD (Thermo Fisher Scientific, Massachusetts, US), and qPCR was performed using a real-time PCR instrument (Thermo Fisher Scientific) according to the manufacturer's protocol. Transcript levels were normalized to those of GAPDH.

### **Transepidermal water loss measurement**

Transepidermal water loss was evaluated using a Vapometer SWL-5001 with a SWL2040-09 probe (Delfin, Kuopio, Finland). HSEs, maintained in tissue culture, exert along with their medium was first acclimatized to ambient conditions of temperature and humidity for at least 15 min before measurement. The same investigator performed all the TEWL measurements. For each HSE, TEWL measurements were performed in triplicate and averaged.

### **Lactate Dehydrogenase (LDH) assay**

LDH-based assays were performed using the Viability/Cytotoxicity Multiplex Assay Kit (Dojindo, Kumamoto, Japan) according to the manufacturer's instructions. For the HSE model, 100 µl of medium was transferred to a 96-well plate and the LDH assay was performed. For cultured human fibroblasts and keratinocytes, 100 µl of the supernatant was transferred to a 96-well plate for further LDH assay after 48 h of treatment with 0.01, 0.1, and 1 µM OMD.

### **Conflict of Interest Statement**

The authors state no conflict of interest. All authors declare they are employee of ROHTO Pharmaceutical Co., Ltd.

### **Acknowledgement**

We would like to thank Professor Adam Butterworth (University of Cambridge, UK) for providing us with the SOMAscan proteomics measurements of 3,301 human plasma samples from the INTERVAL cohort.

Participants in the INTERVAL randomized controlled trial were recruited with the active collaboration of NHS Blood and Transplant England ([www.nhsbt.nhs.uk](http://www.nhsbt.nhs.uk)), which has supported field work and other elements of the trial. DNA extraction and genotyping was co-funded by the National Institute for Health Research (NIHR), the NIHR BioResource (<http://bioresource.nihr.ac.uk>) and the NIHR [Cambridge Biomedical Research Centre at the Cambridge University Hospitals NHS Foundation Trust] [\*]. The INTERVAL study was funded by NHSBT (11-01-GEN). The academic coordinating centre for INTERVAL was supported by core funding from: NIHR Blood and Transplant Research Unit in Donor Health and Genomics (NIHR BTRU-2014-10024), UK Medical Research Council (MR/L003120/1), British Heart Foundation (SP/09/002; RG/13/13/30194; RG/18/13/33946) and the NIHR [Cambridge Biomedical Research Centre at the Cambridge University Hospitals NHS Foundation Trust] [\*]. Proteomic assays were funded by the academic coordinating centre for INTERVAL and MRL, Merck & Co., Inc. A complete list of the investigators and contributors to the INTERVAL trial is provided in reference [\*\*]. The academic coordinating centre would like to thank the blood donor center staff and blood donors for participating in the INTERVAL trial.

This work was supported by the Health Data Research UK, which is funded by the UK Medical Research Council, Engineering and Physical Sciences Research Council, Economic and Social Research Council, Department of Health and Social Care (England), Chief Scientist Office of the Scottish Government Health and Social Care Directorates, Health and Social Care Research and Development Division (Welsh Government), Public Health Agency (Northern Ireland), British Heart Foundation, and Wellcome.

\*The views expressed are those of the authors and not necessarily those of the NHS, the NIHR or the Department of Health and Social Care.

\*\*Di Angelantonio E, Thompson SG, Kaptoge SK, Moore C, Walker M, Armitage J, Ouwehand WH, Roberts DJ, Danesh J, INTERVAL Trial Group. Efficiency and safety of varying the frequency

of whole blood donation (INTERVAL): a randomized trial of 45,000 donors. Lancet. 2017 Nov 25;390(10110):2360-2371.

## References

1. Conboy, I. *et al.* (2005). Nature, 433(7027), 760–764.
2. Lehallier, B. *et al.* (2019). Nature medicine, 25(12), 1843–1850.
3. Zhang, S., & Duan, E. (2018). Cell transplantation, 27(5), 729–738.
4. Cracowski, J. L., & Roustit, M. (2020). Comprehensive Physiology, 10(3), 1105–1154.
5. Egawa, G. *et al.* (2013). Scientific reports, 3, 1932.
6. Leng, L. *et al.* (2020). Journal of tissue engineering, 11, 2041731420972310.
7. Di Angelantonio, E. *et al.*, & INTERVAL Trial Group (2017). Lancet (London, England), 390(10110), 2360–2371.
8. Sun BB, Maranville JC, Peters JE, et al. Nature 2018;558:73-79.
9. Tashima, T. *et al.* (2018). Communications biology, 1, 33.
10. Papadaki, V. *et al.* (2020). Cancers, 12(11), 3362.
11. Kawada, M. *et al.* (2006). International Journal Of Oral-Medical Sciences, 4(3), 170-176.
12. Lin, W. *et al.* (2021). Cell death & disease, 12(2), 147.
13. Ji, M. X., & Yu, Q. (2015). Chronic diseases and translational medicine, 1(1), 9–13.
14. Møller, A. *et al.* (2020). Bone research, 8, 27. <https://doi.org/10.1038/s41413-020-0102-7>
15. Mo, R. *et al.* (2007). Biochemical and biophysical research communications, 353(1), 189–194.
16. Herman, J. *et al.* (2013). Advances in Dermatology and Allergology, 30(6), 388–395.
17. Ohta, H. *et al.* (1998). Maturitas, 30(1), 55–62.
18. Bradshaw, A. D. *et al.* (2003). The Journal of investigative dermatology, 120(6), 949–955.
19. Piérard, G. E. *et al.* (1995). Journal of the American Geriatrics Society, 43(6), 662–665.
20. Wang, H. *et al.* (2018). Journal of biomedical optics, 23(3), 1–4.
21. McCabe, M. C. *et al.* (2020). Matrix biology plus, 8, 100041.
22. Lavker R. M. (1979). The Journal of investigative dermatology, 73(1), 59–66.
23. Neil, J. E. *et al.* (2020). Scientific reports, 10(1), 21192.
24. Roth, W. *et al.* (2012). Journal of cell science, 125(Pt 22), 5269–5279.

## Supplementary

**Supplementary Figure 1.** Effect of OMD on the viability of NHDFs and NHEKs. NHDF (A) and NHEK (B) were treated with medium (Control) and OMD with varying concentrations (0.01 µM, 0.1 µM, and 1 µM) for 48 hours, and cell viability was determined by lactate dehydrogenase (LDH) assay. No significant increase in LDH detection with OMD treatment was observed in both NHDF and NHEK. (C) HSE model was treated with 1 µM OMD for 5 days, and LDH assay showed no significant increase in LDH detection compared with control group.

